

## Measurement of the Line-Reversed Reactions $\bar{p}p \rightarrow \pi^- \rho^-$ and $\pi^- p \rightarrow p \rho^-$ at 6 GeV/c

D. R. Green, R. M. Edelstein, H. J. Halpern,<sup>(a)</sup> E. J. Makuchowski, J. S. Russ, and N. A. Stein<sup>(b)</sup>  
*Carnegie-Mellon University, Pittsburgh, Pennsylvania 15213*

and

Z. Bar-Yam, J. P. Dowd, W. Kern, J. J. Russell, N. Sharfman, and M. N. Singer  
*Southeastern Massachusetts University, New Bedford, Massachusetts 02747*  
 (Received 23 September 1977)

Differential cross sections and density-matrix elements in  $\rho^-$  decay have been measured at 6 GeV/c for  $\bar{p}p \rightarrow \pi^+ \rho^-$  and its line-reversed partner  $\pi^- p \rightarrow p \rho^-$  in the range  $t_{\min} < t < -1.5$  (GeV/c)<sup>2</sup>. The reactions satisfy line-reversal symmetry and the  $\rho^-$  decay is consistent with isotropy for  $-t \lesssim 0.5$  (GeV/c)<sup>2</sup>. For  $-t \gtrsim 0.5$  (GeV/c)<sup>2</sup>, the differential cross sections show a weaker  $t$  dependence, and the decays become anisotropic.

The line-reversed reactions (1)  $\bar{p}p \rightarrow \pi^+ \rho^-$  and (2)  $\pi^- p \rightarrow p \rho^-$  proceed via  $\Delta$  exchange in the  $t$  channel.<sup>1</sup> A simple Regge-pole model<sup>2</sup> would predict identical angular-distribution shapes and  $\rho^-$  density-matrix elements for the two reactions. Furthermore, such models relate Reactions (1) and (2) to other pure  $\Delta$ -exchange reactions such as (3)  $\bar{p}p \rightarrow \pi^+ \pi^-$  and (4)  $\pi^- p \rightarrow p \pi^-$ .

We report here new data on Reactions (1) and (2) at 6 GeV/c and compare them to the line-reversal prediction. At 6 GeV/c, correcting for two-body phase space<sup>3</sup> and scaling to the same available  $s$ ,<sup>4</sup> the line-reversal prediction is<sup>5</sup>  $d\sigma(\bar{p}p \rightarrow \pi^+ \rho^-)/dt = 0.51 d\sigma(\pi^- p \rightarrow p \rho^-)/dt$ . We also comment on the comparison between Reactions (1) and (2) and Reactions (3) and (4) using our measurements of Reactions (3) and (4) at 6 GeV/c reported<sup>6</sup> elsewhere. The simultaneous measurement of Reactions (1)–(4) provides a powerful constraint on the  $\Delta$  trajectory used to describe these processes. For example, different forms of the  $\Delta$  trajectory which give adequate fits to the differential cross sections yield quite different predictions for the density-matrix elements in  $\rho^-$  decay.<sup>7</sup> In addition, absorption effects may alter the relative normalization and affect the density-matrix elements particularly at large momentum transfer, as in the case of forward  $\rho$  production.<sup>8</sup>

These data represent a preliminary sample [40% for (1) and 100% for (2)] of our data set at 6 GeV/c. They are part of a comprehensive study of two-body and quasi-two-body reactions which proceed via baryon exchange at 4, 6, and 8 GeV/c. Previously<sup>6,9</sup> we have presented data on  $\bar{p}p \rightarrow \pi^+ \pi^-$  and  $\pi^- p \rightarrow p \pi^-$ .

The experiment was performed at the Brookhaven National Laboratory multiparticle spectrometer (MPS). Experimental details of the set-

up are given in Ref. 9. For these data additional spark chambers downstream of the MPS magnet were employed to reduce the momentum error on the forward track to  $\delta p/p = \pm 1\%$ . The spark chambers subtended nearly the complete solid angle, so that the  $\rho^-$ -decay angular distribution was essentially unbiased. However, at present the pattern-recognition algorithm misses some tracks going parallel to the field lines. For this reason a cut of  $\pm 0.025$  rad was made in azimuthal angle about the vertical (field) direction, up and down.

The triggers for Reactions (1) and (2) were identical save for Cherenkov counter requirements identifying the incident and forward-scattered particles. Other trigger requirements were identical to those of Ref. 6. In the analysis, only one slow recoil track was allowed in order to reduce multiparticle background. Losses because of accidental extra tracks were determined using forward-elastic-scattering data, which were taken simultaneously. Events were required to be noncoplanar by  $\geq 15$  mrad in order to exclude events from Reactions (3) and (4) from the sample.

The recoil mass,  $M$ , and four-momentum transfer,  $t$ , were calculated from the forward- and beam-track information.  $M^2$  spectra for Reactions (1) and (2) are shown in Fig. 1. A prominent  $\rho^-$  signal is evident in both cases. These spectra were fitted with a Gaussian  $\rho$  distribution plus a polynomial background. The resulting  $\rho$  mass and width, which were insensitive to the order of the polynomial, were consistent with accepted values<sup>10</sup> modified by experimental resolution, as determined from the forward elastic scattering.

The  $\rho$  parameters were then fixed and fits were made to the  $M^2$  spectra for various  $t'$  ( $t' \equiv t - t_{\min}$ )

TABLE I. Corrections to the data.

Correction	$\pi^- p \rightarrow p \rho^-$ (%)	$p p \rightarrow \pi^+ \rho^-$ (%)
Beam reconstruction	$20 \pm 0.5$	$22 \pm 0.5$
Beam leptons	$4 \pm 2$	$0 \pm 0$
Absorption	$13 \pm 1.5$	$18 \pm 1.5$
Decay	$0 \pm 0$	$1 \pm 0.5$
Track reconstruction	$10 \pm 10$	$10 \pm 10$
Single forward track	$12 \pm 2$	$12 \pm 2$
Single recoil track	$9 \pm 4$	$9 \pm 4$
Forward Cherenkov	$1 \pm 0.5$	$4 \pm 1$
Cuts	$5 \pm 2$	$5 \pm 2$

bins, assuming a  $\rho$  signal plus a second-order-polynomial background. Reaction (1) [(2)] yielded  $222 \pm 33$  [ $248 \pm 25$ ] events. The fits were acceptable in all  $t'$  bins. We emphasize that relative systematic errors between (1) and (2) are minimized by the similarity of the trigger and analysis procedure. Additional systematic corrections ( $t'$  independent) are summarized in Table I. However, because of the uncertainty in the form of the background, a conservatively estimated overall normalization error of  $\pm 30\%$  has been assigned. The geometric acceptance as a function of  $t'$ ,  $\theta$ , and  $\varphi$  was determined by the Monte Carlo technique where  $\theta$  and  $\varphi$  are the decay angles of the  $\pi^-$  in the Jackson frame as defined in Ref. 4. Differential cross sections corrected for acceptance are shown in Fig. 2 for (1) and (2). For the purpose of these plots isotropic  $\rho^-$  decay was assumed (this procedure is justified below).

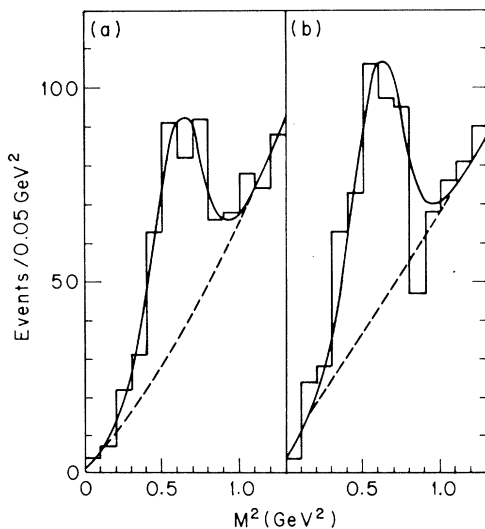


FIG. 1.  $M^2$  spectra fit (solid line) to  $\rho^-$  plus background (dashed line). (a)  $\bar{p}p \rightarrow \pi^+ x$ ; (b)  $\pi^- p \rightarrow p x$ .

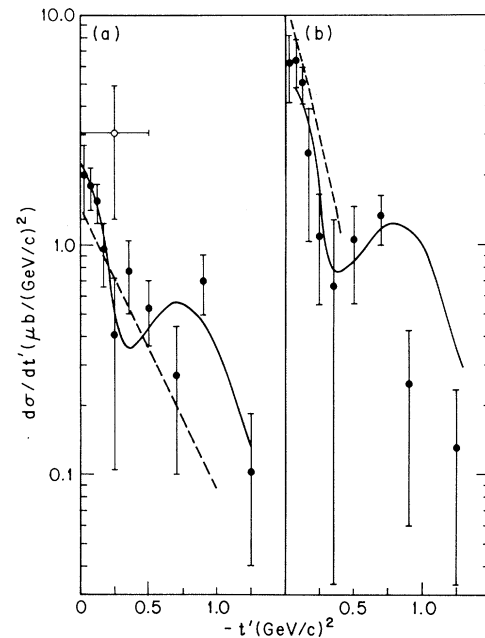


FIG. 2. Differential cross section for (a)  $\bar{p}p \rightarrow \pi^+ \rho^-$  and (b)  $\pi^- p \rightarrow p \rho^-$ . The solid curve in (a) is a fit described in the text. The dashed curve in (a) represents the data of Ref. 6 for  $\bar{p}p \rightarrow \pi^+ \pi^-$ . The solid curve in (b) is the line-reversal prediction using the fit of (a). The dashed curve in (b) is from Ref. 12. The datum point (open circle) in (a) is from Ref. 13.

The most significant features of the data are the following: (a)  $d\sigma/dt'$  varies rapidly with  $t'$  for  $-t' \lesssim 0.5$  ( $\text{GeV}/c$ )<sup>2</sup>. The logarithmic  $t'$  slope is  $\sim 5$  ( $\text{GeV}/c$ )<sup>-2</sup>. (b) The shapes for (1) and (2) are very similar. The smooth curve in Fig. 2(a) is a fit to the form<sup>11</sup>  $d\sigma/dt' = A J_0^2(R_1 \sqrt{-t'}) + B J_1^2(R_2 \sqrt{-t'})$  with  $A = 2.4 \pm 0.7 \mu\text{b}/(\text{GeV}/c)^2$ ,  $B = 3.5 \pm 0.9 \mu\text{b}/(\text{GeV}/c)^2$ ,  $R_1 = 1.1 \pm 0.1$  fm and  $R_2 = 1.1 \pm 0.1$  fm. This fit is also shown in Fig. 2(b) scaled by the line-reversal factor. Clearly for  $-t' \lesssim 0.5$  ( $\text{GeV}/c$ )<sup>2</sup> the line-reversal prediction agrees with the data. (c) For larger  $|t'|$  the data indicate a weaker  $t'$  dependence in both Reactions (1) and (2). This is indicated by the fact that fitting with a simple exponential to the entire  $t'$  range yields shallower logarithmic slopes than for  $|t'| \leq 0.5$  ( $\text{GeV}/c$ )<sup>2</sup>,  $1.70 \pm 0.32$  ( $\text{GeV}/c$ )<sup>-2</sup> for Reaction (1) and  $2.84 \pm 0.35$  ( $\text{GeV}/c$ )<sup>-2</sup> for Reaction (2), and significantly poorer fits, for which the  $\chi^2$  per degree of freedom is 1.6. A break in the  $t$  distribution is predicted by a strong-absorption model, which fitted a variety of baryon exchange data.

For Reaction (2) accurate data exist<sup>12</sup> at 8  $\text{GeV}/c$  for  $-t' \lesssim 0.4$  ( $\text{GeV}/c$ )<sup>2</sup>. With use of  $s^{-2}$  scaling, these data agree well with the present data both

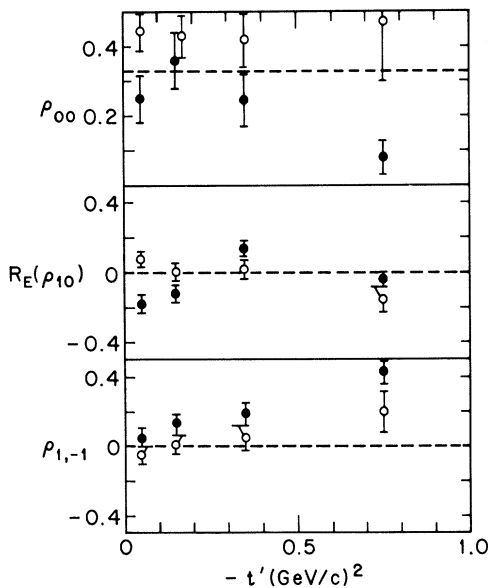


FIG. 3. Density-matrix elements for  $\rho^-$  decay in  $\bar{p}p \rightarrow \pi^+p^-$  (closed circles) and  $\pi^-p \rightarrow p\rho^-$  (open circles). The dashed lines indicate isotropic decay.

in shape and normalization as indicated in Fig. 2(b). Previous measurements of Reaction (1) exist at 5 GeV/c<sup>4</sup> and 8 GeV/c,<sup>13</sup> although with very poor statistics ( $\approx 30$  events). Within the large errors, the agreement with our data is adequate.

The  $\rho^-$  density-matrix elements<sup>14</sup> were fitted as a function of  $t'$  using the Monte Carlo efficiency and the maximum-likelihood method. All data with  $0.3 < M^2 < 0.9$  GeV<sup>2</sup> were used so that roughly equal numbers of background and  $\rho^-$  events were included. Background events, defined as  $0.9 < M^2 < 1.3$  GeV<sup>2</sup>, were consistent with isotropy for both reactions. The results are shown in Fig. 3 where the errors are statistical only. They are consistent with isotropic decay at small  $t'$  for Reactions (1) and (2) although one cannot rule out some angular dependence because it is difficult to estimate interference effects reliably with the large background. Also, for  $-t' \lesssim 0.5$  (GeV/c)<sup>2</sup> they provide another independent verification of line-reversal invariance. For  $-t' \gtrsim 0.5$  (GeV/c)<sup>2</sup>, the angular distribution is anisotropic. In particular  $\rho_{1,-1}$  increases smoothly with  $-t'$ . In the context of strong-absorption models,<sup>8</sup> one can interpret both the weaker  $t'$  dependence and the anisotropic decay for  $-t' > 0.5$  (GeV/c)<sup>2</sup> as due to the increasing importance of absorptive terms at large  $-t'$ .

Isotropic decay of  $\rho$ 's produced via baryon exchange has been observed in  $\pi^+p \rightarrow p\rho^+$  at 5.2

GeV/c,<sup>15</sup>  $\pi^-p \rightarrow n\rho^0$  at 4 GeV/c,<sup>16</sup> and in  $\pi^+n \rightarrow p\rho^0$  at 6 GeV/c.<sup>17</sup> The previous experiment<sup>4</sup> on  $\bar{p}p \rightarrow \pi^+\rho^-$  at 5 GeV/c had insufficient data for a study of the  $\rho$  decay.

In summary, the  $t'$  distributions for Reactions (1) and (2) have a slope of  $\sim 5$  (GeV/c)<sup>-2</sup> for  $-t' \lesssim 0.5$  (GeV/c)<sup>2</sup> as compared to a slope  $\sim 2.7$  (GeV/c)<sup>2</sup> for Reactions (3) and (4). The dashed line in Fig. 2(a) represents a fit to our data<sup>6</sup> for Reactions (3) and (4). The magnitude of  $d\sigma/dt'$  for Reaction (3) is roughly 40% less than that of Reaction (1) at  $t' = 0.0$  (GeV/c)<sup>2</sup>. All four  $\Delta$ -exchange reactions obey line-reversal predictions for the differential cross sections. At larger  $-t'$  [ $-t' \gtrsim 0.5$  (GeV/c)<sup>2</sup>],  $\rho$  production shows a weaker  $t'$  dependence while  $\pi$  production is featureless. The density-matrix elements for Reactions (1) and (2) provide an additional test of line reversal. Moreover, the data imply that the exchanged  $\Delta$  is unaligned for  $-t' \lesssim 0.5$  (GeV/c)<sup>2</sup> and aligned for  $-t' \gtrsim 0.5$  (GeV/c)<sup>2</sup>. We anticipate that our study of the  $s$  dependence of these reactions will assist in limiting existing models with many free parameters.<sup>8</sup> In particular, the strong-absorption-model prediction<sup>18</sup> of a break in the  $t'$  distribution for Reaction (2) also predicts that this break is  $s$  dependent.

This research was supported in part by the U. S. Energy Research and Development Administration and by the National Science Foundation.

<sup>(a)</sup>Present address: Argonne National Laboratory, Argonne, Ill. 60439.

<sup>(b)</sup>Present address: Searle Diagnostics, Inc., Chicago, Ill. 60614.

<sup>1</sup>We use the convention that the small momentum transfer is from the beam particle to the first-mentioned product.

<sup>2</sup>See, for example, V. Barger and D. Cline, *Phenomenological Theories of High Energy Scattering* (Benjamin, Reading, Mass., 1969).

<sup>3</sup>The asymptotic factor is  $\frac{1}{2}$ . At finite energy, a phase-space and flux correction  $(p_{\pi p}^*/p_{\bar{p}p}^*)^2$  is made where  $p^*$  is the initial-state c.m. momentum.

<sup>4</sup>A. Eide *et al.* [Phys. Lett. **41B**, 225 (1972)] quote  $s^{-2}$  scaling. Under this assumption, the factor in Ref. 3 above becomes  $0.5(p_{\pi p}^*/p_{\bar{p}p}^*)^2(s_{\bar{p}p}/s_{\pi p})^{-2} = 0.51$ , where  $s$  is the square of the c.m. energy.

<sup>5</sup>Other line-reversal predictions can be made; see, e.g., V. Barger and D. Cline, Phys. Lett. **25B**, 415 (1967).

<sup>6</sup>N. Sharfman *et al.*, Bull. Am. Phys. Soc. **22**, 653 (1977).

<sup>7</sup>C. C. Shih, Phys. Rev. Lett. **22**, 105 (1969).

<sup>8</sup>G. L. Kane and A. Seidl, Rev. Mod. Phys. **48**, 309 (1976).

- <sup>9</sup>N. A. Stein *et al.*, Phys. Rev. Lett. **39**, 378 (1977).  
<sup>10</sup>T. G. Trippe *et al.*, Rev. Mod. Phys. **48**, No. 2, pt. 2, S51 (1976).  
<sup>11</sup>M. Ross *et al.*, Nucl. Phys. **23B**, 269 (1970).  
<sup>12</sup>E. W. Anderson *et al.*, Phys. Rev. Lett. **22**, 102 (1969).  
<sup>13</sup>R. M. Edelstein *et al.*, Phys. Rev. Lett. **23**, 433 (1969).  
<sup>14</sup>S. Gasiorowicz, *Elementary Particle Physics* (Wiley, New York, 1967), p. 459.  
<sup>15</sup>P. J. Carlson *et al.*, Phys. Lett. **33B**, 502 (1970).  
<sup>16</sup>P. B. Johnson *et al.*, Phys. Rev. **176**, 1651 (1968).  
<sup>17</sup>A. Engler *et al.*, Phys. Lett. **50B**, 275 (1975).  
<sup>18</sup>R. L. Kelley *et al.*, Phys. Rev. Lett. **24**, 1511 (1970).

## Mass Asymmetry and Total-Kinetic-Energy Release in the Spontaneous Fission of $^{262}\text{[105]}$

C. E. Bemis, Jr., R. L. Ferguson, F. Plasil, R. J. Silva, G. D. O'Kelley, M. L. Kiefer,  
 R. L. Hahn, and D. C. Hensley  
*Oak Ridge National Laboratory, Oak Ridge, Tennessee 37830*

and

E. K. Hulet and R. W. Lougheed  
*Lawrence Livermore Laboratory, Livermore, California 94550*  
 (Received 20 September 1977)

Mass and total-kinetic-energy (TKE) distributions of fission fragments from the spontaneous fission of  $^{262}\text{[105]}$  and  $^{256}\text{Fm}$  have been obtained. No events with anomalously high TKE were observed, contrary to theoretical expectations. The mass distribution from the fission of  $^{262}\text{[105]}$  is very probably asymmetric and similar to distributions obtained from all spontaneously fissioning systems with the exception of  $^{257}\text{Fm}$  and  $^{258}\text{Fm}$ .

Numerous measurements of mass and of total-kinetic-energy (TKE) distributions from spontaneous fission of nuclei with  $92 < Z \leq 100$  have been made in the last fifteen years.<sup>1-9</sup> With the exception of the spontaneous fission of  $^{257}\text{Fm}$  and  $^{259}\text{Fm}$ , the mass distributions were all found to be peaked at asymmetric mass divisions, and the averaged TKE was found to increase gradually with increasing  $Z$ . The monotonic increase in the averaged TKE can be understood in terms of the liquid-drop model,<sup>10</sup> while theoretical calculations indicate<sup>11-21</sup> that shell structure of the nascent fragments and/or shell effects in the region of the second peak in the fission barrier are responsible for the asymmetric mass distributions. In sharp contrast, fission of the heavier fermium isotopes<sup>2,3,9,22</sup> results in mass distributions that are peaked at symmetric mass divisions and in TKE's that show an increase for near-symmetric mass splits. This behavior can also be understood on theoretical grounds<sup>12-15,20</sup> and is qualitatively attributed to the preferred formation of nuclei in the region of the doubly magic  $^{132}_{50}\text{Sn}$  nucleus.

As a consequence of the spherical shape of closed-shell nuclei, Schmitt and Mosel<sup>15</sup> predict substantially increased total kinetic energies (as much as 50 MeV higher than those predicted by semiempirical fission systematics<sup>10</sup>) for fission-

ing systems with  $A$  between about 260 and 275. The practical importance of the validity of Schmitt-Mosel predictions lies in the possible use of high TKE as a signature for superheavy elements and/or elements with  $260 \approx A \approx 275$ . Studies aimed at testing the theory and at determining if symmetric fission occurs for spontaneously fissioning nuclei with  $Z > 100$  are difficult because of the short half-lives of the fissioning species, as well as due to difficulties involved in synthesizing them.  $^{252}\text{No}$  is the only known case studied with  $Z > 100$ , and it was found to have, as expected, an essentially normal TKE and an asymmetric mass distribution.<sup>23</sup> Fission studies of excited compound nuclei are easier, but may not be relevant, since the high excitation energy may eliminate shell effects.<sup>24,25</sup>

We report here results from the fission of  $^{262}\text{[105]}$ , the second heaviest known nuclide. The TKE predicted by Schmitt and Mosel is about 250 MeV for near-symmetric mass splits, while the averaged TKE expected from fission systematics is about 200 MeV. In our experiments the recoiling  $^{262}\text{[105]}$  nuclei, obtained from the reaction  $^{249}\text{Bk}(^{18}\text{O}, 5n)^{262}\text{[105]}$ , were deposited onto 40- $\mu\text{g} \cdot \text{cm}^{-2}$  carbon foils using a helium jet technique.<sup>23</sup> In a given cycle, the target was bombarded for 80 sec; the collection foil was then rotated between two surface-barrier detectors (detectors